Icarus 209 (2010) 854–857

Contents lists available at ScienceDirect

Icarus

journal homepage: www.elsevier.com/locate/icarus

Note

Far-infrared opacity sources in Titan's troposphere reconsidered

R. de Kok [a,*], P.G.J. Irwin [b], N.A. Teanby [b]

[a] SRON Netherlands Institute for Space Research, Sorbonnelaan 2, 3584 CA Utrecht, The Netherlands

[b] Atmospheric, Oceanic & Planetary Physics, Department of Physics, University of Oxford, Clarendon Laboratory, Parks Road, Oxford OX1 3PU, UK

ARTICLE INFO

Article history:
Received 18 February 2010
Revised 12 June 2010
Accepted 23 June 2010
Available online 3 July 2010

Keywords:
Titan
Atmospheres, Composition
Infrared observations

ABSTRACT

We use Cassini far-infrared limb and nadir spectra, together with recent Huygens results, to shed new light on the controversial far-infrared opacity sources in Titan's troposphere. Although a global cloud of large CH_4 ice particles around an altitude of 30 km, together with an increase in tropospheric haze opacity with respect to the stratosphere, can fit nadir and limb spectra well, this cloud does not seem consistent with shortwave measurements of Titan. Instead, the N_2–CH_4 collision-induced absorption coefficients are probably underestimated by at least 50% for low temperatures.

1. Introduction

Titan's troposphere has an active methane cycle that resembles the Earth's hydrological cycle. Unfortunately, there are only a few small regions of the electromagnetic spectrum that can penetrate Titan's atmosphere as deep as the troposphere, making remote sensing of the methane cycle somewhat troublesome. The wavelengths that probe Titan's troposphere include a few narrow windows in the methane absorption in the visible and near-infrared, and the far-infrared, where there are only very few gas absorption lines (Tomasko et al., 2008a). Interpretation of the latter wavelength region (~200–600 cm^{-1}) has proven difficult due to uncertainties in tropospheric opacity sources. Early analysis of Voyager Infrared Interferometer Spectrometer and Radiometer (IRIS) spectra (Thompson and Sagan, 1984; Toon et al., 1988; McKay et al., 1989) invoked methane clouds to account for (part of) the additional opacity needed to fit the data. When more reliable collision-induced absorption (CIA) coefficients became available this additional opacity source was concluded to result from an increase of N_2–CH_4 CIA, caused by supersaturated methane concentrations (Courtin et al., 1995; Samuelson et al., 1997). Furthermore, it was shown by Samuelson et al. (1997) that large ethane particles near the tropopause could also be used to fit the far-infrared spectra, although methane supersaturation was still needed to improve the fit in this case. Courtin et al. (1995) also found a marginal agreement when clouds near the tropopause are included, but they obtained a better agreement with the data by including supersaturation. However, *in situ* measurements by the Huygens probe in early 2005 at 10°S showed tropospheric CH_4 not to be supersaturated at all (Niemann et al., 2005). Since the arrival of Cassini, far-infrared spectra that probe the troposphere have not been analysed in detail again. Hence, the source of the far-infrared tropospheric opacity source remains unknown. Here, we will re-assess the issue of Titan's far-infrared opacity sources, using data from instruments onboard the Cassini mission and strong constraints placed by the Huygens Gas Chromatograph Mass Spectrometer (GCMS) and Atmospheric Structure Instrument (HASI) measurements. This enables us to place new constraints on possible tropospheric opacity sources.

2. Observations

We use far-infrared spectra between 250 and 550 cm^{-1} from the Cassini Composite Infrared Spectrometer (CIRS) (Flasar et al., 2004), with a spectral resolution of 13 cm^{-1}. Below 250 cm^{-1} the spectra probe the tropopause region and more variables come into play (e.g. various haze and cloud signatures (de Kok et al., 2007), trace gas emission lines, and potential errors in N_2–N_2 CIA). Hence, the wavenumber region below 250 cm^{-1} does not add significant constraints on this issue and is not considered. The latitude of these observations (15°S) is close to the latitude of the Huygens landing site, since most variables are constrained by Huygens observations there. We use both a nadir spectrum and six limb spectra with central tangent heights lower than 50 km. The six limb spectra are obtained by fitting splines through radiance versus altitude points at each measured wavenumber of the 119 individual spectra between 0 and 170 km taken during this limb observation (see Teanby, 2007; de Kok et al., 2007). The field-of-view (FOV) of the limb measurements is 53 km, which is taken into account by calculating spectra at five tangent altitudes within the FOV and weighing them according to the spatial response of the CIRS detector (Teanby and Irwin, 2007). The nadir spectrum is an average of 36 spectra taken within several minutes spanning 5° of latitude. Data were taken on 22 July 2006 (nadir) and 7 September 2006 (limb), which are the T16 and T17 Titan flybys. No significant temporal or spatial variations at this latitude are expected in this period and hence all these observations can be fitted simultaneously.

3. Model

We use the NEMESIS radiative transfer code for spectral calculations and retrievals (Irwin et al., 2008). This code uses the correlated-*k* method (Lacis and Oinas, 1991) to calculate spectra and it includes an optimal estimation retrieval algorithm (Rodgers, 2000). When CH_4 clouds are considered, multiple scattering is used, since large CH_4 particles are very effective scatterers in this wavelength region. For the nadir spectrum, a doubling–adding routine is used in a plane-parallel atmosphere (e.g. Plass et al., 1973). For the limb spectra, this doubling–adding routine is used to calculate the internal radiation field, which describes the upward and downward going radiances between each layer at a number of emission angles. The equation of radiative transfer that includes both thermal emission and scattering (Hanel et al., 2003) is then numerically solved in a spherical geometry, using the following

* Corresponding author. Fax: +31 887775601.
E-mail address: R.J.de.Kok@sron.nl (R. de Kok).

0019-1035/$ - see front matter
doi:10.1016/j.icarus.2010.06.035

scattering source function, which is the integral over solid angle Ω of the phase function $P(\theta)$, with phase angle θ, multiplied by the internal radiation field I', scaled by the single-scattering albedo of the atmospheric layer $\tilde{\omega}$:

$$J_s = \tilde{\omega}\frac{1}{4\pi}\int_{4\pi} I'P(\theta)d\Omega \quad (1)$$

Hence, our limb scattering model is a pseudo-spherical approximation, since the internal radiation field is approximated in a plane-parallel atmosphere. The continuum opacity sources are CIA of pairs of N_2, CH_4 and H_2, calculated according to Borysow and Frommhold (1986a,b,c, 1987), Borysow (1991) and Borysow and Tang (1993). Pressures, temperatures and CH_4 volume mixing ratio (VMR) are taken from Huygens GCMS and HASI measurements (Niemann et al., 2005; Fulchignoni et al., 2005). A H_2 VMR of 0.1% is assumed (Courtin et al., 2008). Also, photochemical haze and potentially clouds contribute to the far-infrared opacity. Haze is assumed to be non-scattering, using the extinction cross-sections of de Kok et al. (2007). Haze is expected to be highly absorbing in this wavelength region, due to high imaginary refractive indices and small particle sizes (Khare et al., 1984), and hence the non-scattering nature of the haze particles seems a reasonable assumption. The vertical profile is consistent with the southern profiles of de Kok et al. (2007) and with Tomasko et al. (2008b). Above an altitude of 80 km this profile has a scale height of 65 km, whereas below 80 km the haze scale height is identical to the atmospheric pressure scale height. Solid CH_4 clouds are modelled using Mie theory and the optical constants of Martonchik and Orton (1994). We use a log-normal distribution of particle sizes, with an effective radius of 100 μm and a log(σ) value of 0.3 (after Barth and Toon, 2006). This distribution includes particles sizes between ~40 and 250 μm and results in a flat extinction cross-section between 250 and 550 cm^{-1} and single-scattering albedos close to unity. This behaviour is also seen for similarly broad distributions around mean particle radius larger than 50 μm, so the exact particle size is not well constrained when cloud particles become this large. Similarly, our exact choice of particle size is also of little consequence. For easy computations of the phase function, double Henyey–Greenstein functions are fitted to the Mie results.

4. Results

Using only the known gas and haze opacity, the calculated spectrum is shown as the thin solid line in Fig. 1. This synthetic spectrum clearly overestimates the nadir radiances, meaning that an additional opacity source is needed in the troposphere. We also found that tropospheric opacity was needed when fitting other low latitude nadir data from other flybys. Also the Voyager IRIS data is consistent with the CIRS data, meaning that previous conclusions based on Voyager data were not the result of instrumental artefacts. As the past has shown (e.g. Courtin et al., 1995; Samuelson et al., 1997), far-infrared nadir spectra can be fitted using a range of assumptions. For instance, instead of an increased CH_4 abundance, the N_2–CH_4 CIA coefficient might be in error. Multiplying the coefficients by a factor of 1.5 gives excellent agreement with nadir observations at low latitudes (Tomasko et al., 2008a), which is also shown in Fig. 1 (dotted lines). This additional opacity causes one to probe higher in the troposphere, where temperatures are lower, giving rise to lower radiances. However, Fig. 1 also shows that the limb measurements are poorly reproduced with this assumption. We find that we cannot fit the limb spectra by only scaling the N_2–CH_4 CIA coefficients, even if we scale different altitudes differently. This is because the higher limb spectra probe high in the troposphere, where atmospheric density (and thus CIA opacity) is low, reducing the sensitivity to CIA. The atmosphere is optically thin there and hence adding opacity will increase radiances. At present, we cannot rule out large temperature-dependent and wavelength-dependent errors on the N_2–CH_4 CIA coefficients of Borysow and Tang (1993).

Alternatively, we can fit the limb measurements reasonably by increasing tropospheric haze opacity in the upper troposphere by a factor of 5 or more compared to our nominal model (see Fig. 2). However, such an increase in haze opacity does little to reduce the nadir radiances. A combination of increased CIA and increased tropospheric haze opacity can fit both limb and nadir data reasonably well (see Fig. 1, long dashed lines).

A third plausible variable is a potential global CH_4 cloud. We retrieved a cloud profile by allowing the cloud density to vary between altitudes of 20 and 40 km. If only this cloud is retrieved, nadir radiances can be brought to the correct magnitudes using a thin cloud around 30 km (see Fig. 2), although the limb spectra are not fitted very well. Adjusting the haze opacity as well yields good fits to all spectra (see Fig. 1, dot-dashed lines). Again, haze opacity in the high troposphere has to be increased in this case (see Fig. 2).

5. Discussion

We have shown that large CH_4 cloud particles at 30 km can be used to fit far-infrared nadir spectra that probe Titan's troposphere. An increase in tropospheric haze opacity with respect to our nominal model is needed to fit the limb spectra. Based on Huygens temperature (HASI) and CH_4 (GCMS) measurements, Tokano et al. (2006) and Barth and Toon (2006) show that a global CH_4 cloud should exist

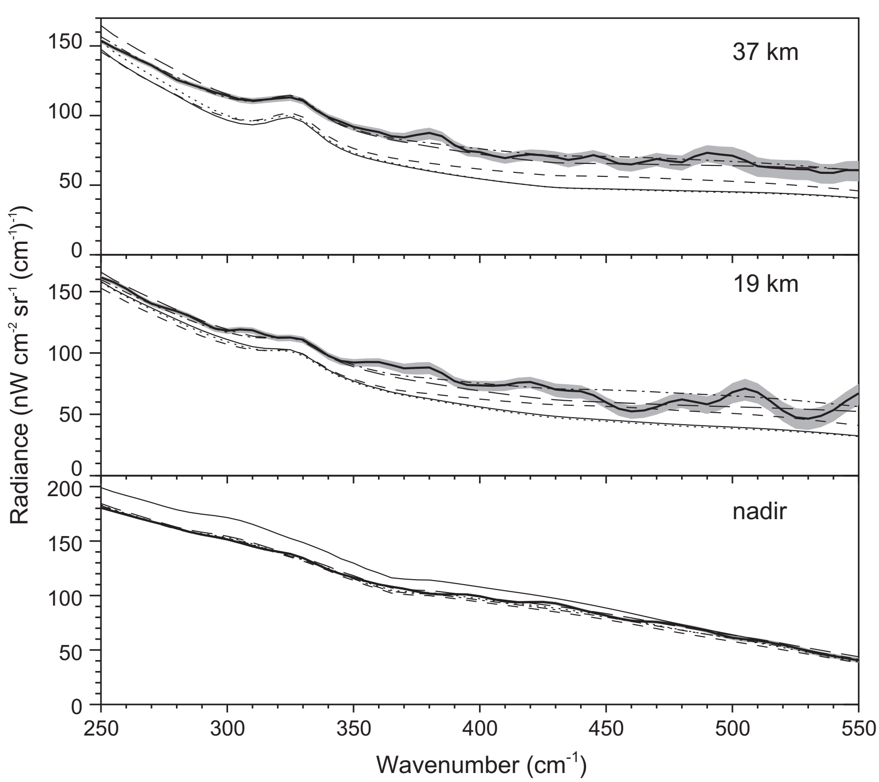

Fig. 1. Fits (thin lines) to three of the measured spectra (thick solid lines) for different model cases (thin solid line – nominal case based on Huygens results; dotted line – scaled N_2–CH_4 CIA; short dashed line – retrieved CH_4 cloud; dot-dashed line – retrieved CH_4 cloud and haze profiles; long dashed line – retrieved haze profile and scaled N_2–CH_4 CIA). For the limb observations the tangent height at the centre of the detector is shown. Error bars are shown as shaded areas.